Vibrational Analysis of Polyaniline: A Model Compound Approach

M.-I. Boyer,*,† S. Quillard,† E. Rebourt,‡ G. Louarn,† J. P. Buisson,† A. Monkman,‡ and S. Lefrant†

Institut des Matériaux de Nantes, Laboratoire de Physique Cristalline, B.P. 32229, 44322 Nantes, France, and Electroactive Organic Materials Research Group, Department of Physics, University of Durham, South Road, Durham DH1 3LE, U.K.

Received: August 13, 1997; In Final Form: February 18, 1998

In this work, we have used an oligomer model compound approach for the understanding of the vibrational spectra of the principal forms of polyaniline. Selected model compounds have been studied by Raman and infrared (IR) spectroscopies. The observed vibrational bands are assigned to the expected modes, by revealing the relationships between molecules. In a more theoretical part, dynamical calculations on the different model compounds and their related polymers are presented. The use of model compounds allows us to reach better sets of force constants, as soon as we assume that the parameters can be transferred to the polymeric forms. The obtained values of these force constants are discussed in regards to the oxidation state of polyaniline and its corresponding geometrical structure.

1. Introduction

Polyaniline is one of the most extensively studied conducting polymers[1] mainly due to its stability and processability, which, in turn, facilitates its potential applications.[2−4] Polyaniline exists in three principal forms: leucoemeraldine (totally reduced), emeraldine (semioxidized), and pernigraniline (totally oxidized). The two latter forms exhibit a rather complicated molecular structure in which oxidized and reduced units coexist.

In addition to render polyaniline conductive, it is necessary either to oxidize leucoemeraldine or to protonate emeraldine in order to form so-called "semiquinone radical structure", which favors conductivity. This conversion involves a drastic change in the electronic structure of the polymer.

It is known that vibrational spectroscopy is extremely sensitive to the electronic structure changes in polyaniline. Thus by using infrared and Raman, one can easily register all interconversions between different states of polyaniline involving both oxidation and protonation processes.

To facilitate the assignment of the observed vibrational modes, we have adopted the so-called "model compound approach" already used by Furukawa et al. and Quillard et al. in the case of the phenyl-end-capped dimer and its imine form.[6−9] In this approach, we start our vibrational analysis with small molecules of known geometry whose constituting units mimic those of different types of polyaniline. In many cases, the vibrational features[10] as well as other properties[11,12] of polyaniline and other conductive polymers have been correctly predicted by the extrapolation of the data obtained for the oligomer model compounds.

In our initial study,[13] we have investigated the vibrational properties of three model compounds of leucoemeraldine (aniline, diphenylamine, and a phenyl-end-capped dimer called B3 in our convention). Since the quality of the oligomer approach improves as the length of the oligomer studied increases,[14] in this research we have extended our investigations to the longest molecules such as the phenyl-end-capped tetramer (B5) and hexamer (B7). Furthermore, we have studied oxidized phenyl-end-capped tetramers containing two (B4Q1) and four (B3Q2) imine nitrogens. These two compounds can be considered as model compounds of emeraldine and pernigraniline, respectively. The imine form of the phenyl-end-capped dimer (B2Q1), a model compound of pernigraniline base, has also been the subject of a vibrational study. All oligomers studied are depicted schematically in Figure 1.

Thus the main goal of the research presented here was to verify the previous assignment of the vibrational modes on the basis of the better model oligomers and to calculate more precisely the set of force constants for neutral (basic) forms of leucoemeraldine (LB), emeraldine (EB), and pernigraniline (PB).

2. Experimental Section

A. Synthesis. Phenyl-end-capped dimer was purchased from Aldrich, purified, and crystallized by vacuum sublimation. Colorless crystals have been obtained. Phenyl-end-capped tetramer and hexamer in their reduced leucoemeraldine forms were prepared via a modified Honzl route[15−17] and unequivocally identified by ^{13}C NMR spectroscopy.[18] Emeraldine base phenyl-end-capped tetramer was obtained by oxidation of its leucoemeraldine base form with silver(I) oxide in THF. It consisted of a 70/30 mixture of two isomers. All oligomer samples were powders except for B3 (crystals).

B. Spectroscopic Investigations. Methanol solution UV−vis−NIR spectra of the oligomers were recorded on a Varian Cary 2300.

Infrared absorption experiments were made on a FTIR spectrometer (Nicolet 20 SXC) with a DTGS detector. The spectra were registered at room temperature using KBr pellets technique. A 4 cm^{-1} spectral resolution was taken for all the IR experiments, and the spectra were corrected for the substrate absorption.

Raman spectra obtained with the excitation lines in the visible range (457.9, 514.5, 676.4 nm) were recorded using a microscope on a multichannel Jobin Yvon T64000 spectrometer connected to a CCD detector (resolution ca. 10 cm^{-1}). The scattering signal was collected at 90°. The spectra were

* E-mail: BOYER@CNRS-IMN.FR.
† Institut des Matériaux de Nantes.
‡ University of Durham.

S1089-5647(97)02652-7 CCC: $15.00
Published on Web 08/27/1998

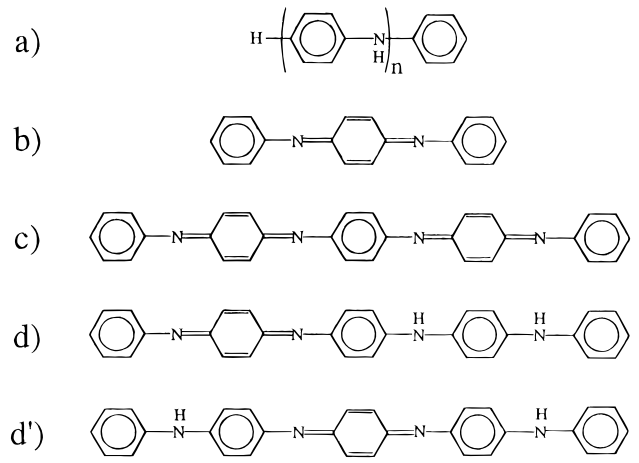

Figure 1. Schematic structure of the model compounds under study: (a) $n = 2$, phenyl-end-capped dimer (B3 called PCD in ref 5); $n = 4$, phenyl-end-capped tetramer (B5); $n = 6$, phenyl-end-capped hexamer (B7); (b) imine form of phenyl-end-capped dimer (B2Q1); (c) pernigraniline base phenyl-end-capped tetramer (B3Q2); and (d, d′) emeraldine base phenyl-end-capped tetramer (B4Q1) (B, benzenoid ring; and Q, quinoid ring).

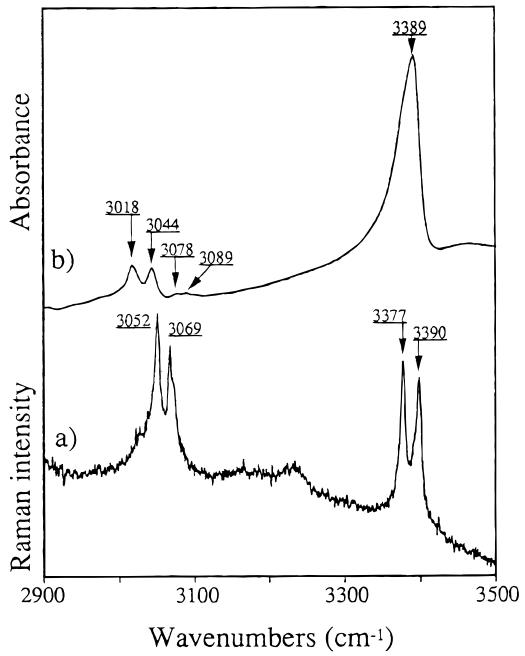

Figure 2. (a) Raman ($\lambda_{exc} = 457.9$ nm) and (b) infrared spectra of B5 in the frequency range 2900−3500 cm^{-1}.

registered at liquid nitrogen temperature (77 K), and the power beam was limited to 20 mW, in the case of the reduced molecules, and to about 1 mW in the case of the oxidized ones, to avoid the problem of degradation, which can occur at room temperature.

For the 1064 nm excitation wavelength, a FT-Raman Bruker RFS 100 spectrometer was used in a backscattering configuration. Typical resolution in the FT-Raman spectra was 4 cm^{-1}.

3. Results and Discussion

A. Reduced Model Compounds of Polyaniline. The Raman and infrared spectra of model compounds of leucoemeraldine base (i.e., the reduced form of polyaniline) are displayed in Figures 2 and 3. The Raman spectrum of the phenyl-end-capped dimer depicted in Figure 3 differs slightly from those presented by Furukawa et al. and Quillard et al.[9] Indeed, our Raman study has been performed on samples purified and recrystallized from as-made Aldrich product (gray powder). The other Raman spectra have been obtained on this gray powder. The main differences concern the bands assigned to the symmetric C−N−C stretching and to the C−H bending.

For simplicity in the subsequent text, the Wilson notation, established for benzene and its derivatives, will be used. The most characteristic spectral regions will be discussed separately, and the vibration modes originating from the terminal rings will be separated (when possible) from those characteristic of the inner chain units. The assignments of the experimentally measured bands are collected in Tables 1 and 2.

Raman and IR spectra of leucoemeraldine base have already been published.[5,19] They exhibit the following Raman and IR-active bands:

Raman 1618, 1597, 1219, 1181 868, and 603 cm^{-1}

IR 1596, 1496, 1282, 1218, 1167, 1107, 1008, and 814 cm^{-1}

In the subsequent text, we will frequently refer to these modes.

(a) Region I: 3000−3500 cm^{-1}. At these wavenumbers two types of modes are expected: the C−H and the N−H stretchings. The C−H stretchings originating from the aromatic ring are clearly visible at 3052, 3069, and 3072 cm^{-1} in the Raman spectrum of phenyl-end-capped tetramer (B5) (Figure 2). In the IR spectrum these vibrations give rise to broad bands at 3018, 3044, 3078, and 3089 cm^{-1}. Two sharp Raman peaks observed at 3377 and 3390 cm^{-1} correspond to the N−H symmetric stretching. Their asymmetric homologue induces one band observed at 3389 cm^{-1} in the infrared spectrum of B5. In the infrared spectrum of the polymer, we see only two bands in this spectral range, located at 3020 and 3376 cm^{-1}, attributed to C−H and N−H stretching, respectively.

(b) Region II: 1100−1700 cm^{-1} (C−C Stretching − C−H Bending Vibrations). In this frequency range, C−C stretching (skeletal modes) and C−H bending vibrations are expected in the Raman and infrared spectra of molecules or macromolecules containing aromatic rings. The Raman spectra of the model compounds under study and leucoemeraldine base (LB) are characterized by an intense band at about 1618 cm^{-1} with a distinct shoulder at lower frequency which can be deconvoluted into several satellites. The 1600 cm^{-1} vibrations mainly involve "quadrant stretching" of the ring C−C bonds with a partial contribution of the in-plane C−H bending (vibrational modes 8a and 8b). Indeed, for benzene this Raman mode (8a,b in Wilson notation) at 1596 cm^{-1} is doubly degenerate (E_{2g}). So, in the oligomers of polyaniline, the substitution splits this mode into two components: 8a and 8b. However, spectral lines corresponding to these modes are very close in frequency, which makes them difficult to differentiate. We assign the intense line to the 8a mode of the inner rings. According to the extensive literature dealing with the vibrational characteristics of the benzene derivatives, in mono- and para-disubsituted derivatives of benzene, the vibrational mode 8a is expected at higher frequency than the 8b mode. Furthermore, the 8a mode of the monosubstituted derivatives of benzene is located at about 1600 cm^{-1} (at 1603 cm^{-1} in the Raman spectrum of diphenylamine, i.e., B2 in our nomenclature) and shifts toward the high frequency when the aromatic rings are paradisubstituted (B3, B5, and B7) at about 1620 cm^{-1}. The intensity of the contributions due to the outer rings decreases (see 993 cm^{-1} for example) when the chain length increases, which confirms this assignment. Consequently, the 8b mode of the inner ring

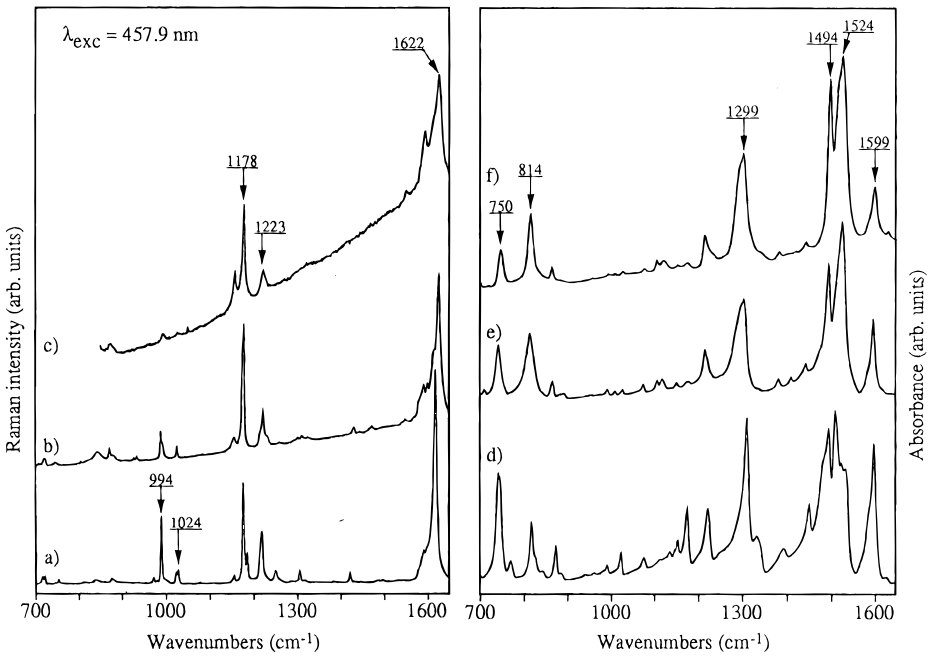

Figure 3. Raman spectra (λ_{exc} = 457.9 nm) of (a) B3, (b) B5, and (c) B7 and infrared spectra of (d) B3, (e) B5, and (f) B7, in the frequency range 700−1650 cm^{-1}.

TABLE 1: Experimental and Calculated Raman Band Wavenumbers/cm^{-1} of Leucoemeraldine Base and Its Model Compounds (Excited at 457.9 nm), Potential Energy Distribution (PED) of B3, and Vibrational Assignment of the Raman Bands[a]

						Leucoemeraldine base					
Wilson	B3 A_g		B5 A_g		B7 A_g	A_g		B_{3g}		PED (%)	
notation	expt	calc	expt	calc	expt	expt	calc	expt	calc	obtained on B3	vibrational assignment
8a	1620	1619	1624/1614	1620/1618	1622	1618	1617	1606	1614	41 K_t + 29 $K_{t'}$ + 27 H_ϕ	C−C stretch. ring
8a	1603	1614	1600	1614						52 K_t + 28 H_ϕ + 18 $K_{t'}$	C−C stretch. ring
8b	1594	1604	1592	1604						45 $K_{t'}$ + 32 K_t + 20 H_ϕ	C−C stretch. ring
8b	1584	1593	1584/1550	1599/1590		1597	1603	/	1582	68 $K_{t'}$ + 16 H_ϕ	C−C stretch. ring
19a			/	1523							
19a	1501	1502	/	1502						58 H_ϕ + 21 K_t + 16 $K_{t'}$	C−H bend. ring + C−C stretch.
19b	1491	1460	1474	1461						53 H_ϕ + 26 K_t	C−H bend. ring + C−C stretch.
19b			/	1441							
N−H	1426	1427	1431	1427/1425				/	1424	91 H_δ	C−N−H bend.
3	1321	1334	1329	1334						96 H_ϕ + 11 K_t	C−H bend.
3	1310	1312	1314/1304	1315/1306		/	1311	/	1297	86 H_ϕ	C−H bend.
14	1293	1275	/	1279						61 H_ϕ + 43 $K_{t'}$ + 21 K_t	C−H bend.
C−N	1256	1250	1264	1256/1249				/	1248	69 K_R + 16 H_ϕ	asym. C−N stretch.
			1234	1240							
C−N	1223	1221	1225/1220	1225/1219	1223	1219	1219			43 K_R + 25 H_ϕ + 12 $K_{t'}$	sym. C−N stretch.
9a	1189	1180	/	1179						69 H_ϕ + 17 K_t	C−H bend.
9a	1182	1172	1180	1174/1170	1178	1181	1169	/	1175	55 H_ϕ + 27 K_t	C−H bend.
15	1160	1156	1159	1156						80 K_t + 27 H_ϕ − 26 $F^o_{(t,t)}$	C−H bend. + C−C stretch.
18b			/	1116							
18b	1082	1080	/	1080						44 K_t + 41 H_ϕ	C−H bend. + C−C stretch.
18a	1030	1028	1028	1028						32 H_ϕ + 29 K_t + 16 H_α	C−H bend. + ring def.
18a			1020	1024							
1 + 12	995	989	993	989	994					39 K_t + 25 H_α + 13 $F^o_{(t,t)}$	ring def.
1	882	888	882/874	896/877	873	868	872	/	898	49 $K_{t'}$+ 13 $F^o_{(t,t)}$ + 13 K_R	ring def.
amine	843	823	846	826						29 H_α+ 23 $K_{t'}$+ 17 K_R	
			746	748							
6a	660	650	666	659		667	668			40 H_α +26 $H_{\delta'}$ +13 $H_{\phi'}$	C−N−C bend.
6b	620	607	600	620/607		603	606	/	607	62 H_α +15 H_ϕ + 12 $K_{t'}$	C−C−C bend.
6b	607	601		604						48 H_α +16 $H_{\phi'}$ + 12 H_ϕ	C−C−C bend.

[a] Only the three main PED (>10%) are given (/ not observable).

and 8a and 8b mode of the terminal rings are located within the shoulder of the intense band.

Theoretically, in paradisubstituted phenylene rings these "quadrant vibrations" should be IR inactive because all atoms in para positions with respect to each other move in exactly opposite directions. However, these modes centered on the terminal rings are IR active and visible in the spectra at 1600 cm^{-1}. These vibrations are of great importance in the polymers, because they are very sensitive to the chemical character (quinonoid/semiquinoid/aromatic) of the ring.

In substituted benzenes, the E_{1u} degenerate vibration, which absorbs at 1486 cm^{-1}, also splits into two bands (19a,b). This

TABLE 2: Experimental and Calculated Infrared Band Wavenumbers/cm^{-1} of Leucoemeraldine Base and Its Model Compounds (Excited at 457.9 nm), PED of B3, and Vibrational Assignment of the Infrared Bands

						Leucoemeraldine base					
Wilson	B3 B_u		B5 B_u		B7 B_u	B_{1u}		B_{2u}		PED (%)	
notation	expt	calc	expt	calc	expt	expt	calc	expt	calc	obtained on B3	vibrational assignment
8a			1597	1619	1599						
8a	1599	1614	/	1614						53 K_t + 28 H_ϕ + 18 $K_{t'}$	C−C stretch. ring
8b	1590	1602	/	1603						40 K_t + 35 $K_{t'}$ + 23 H_ϕ	C−C stretch. ring
8b			1587	1594	1583						
19a	1524	1523	1524	1524/1522	1523	sh.	1522	1496	1518	51 H_ϕ + 38 $K_{t'}$ + 16 K_R	C−C stretch. + C−H bend. ring
19a	1494	1502	1493	1502	1496					58 H_ϕ + 21 K_t + 16 $K_{t'}$	C−C stretch. + C−H bend. ring
19b	1486	1461	/	1461						53 H_ϕ + 26 K_t	C−C stretch. + C−H bend. ring
19b	1450	1441	1442	1442/1440	1442	/	1433	/	1420	55 K_δ + 23 H_ϕ + 14 K_t	C−H bend. + N−H bend.
amine	/	1427	1410	1427/1425	1419			/	1442	40 H_δ + 33 H_ϕ + 26 K_t	C−H bend. + N−H bend.
3	1334	1334	/	1334						96 H_ϕ + 11 K_t	C−H bend.
3			/	1312							
14	/	1284	/	1281						55 H_ϕ + 53 $K_{t'}$ + 27 K_t	C−H bend. + C−C stretch.
C−N	1253	1256	1248	1259/1256				/	1258	57 K_R + 23 H_ϕ + 16 $K_{t'}$	asym. C−N stretch.
14	/	1239	/	1250		1282	1272	/	1226	54 $K_{t'}$ + 26 H_ϕ + 22 K_R	C−H bend. + C−C stretch.
C−N	1224	1227	1216	1230/1228		1218	1232			89 $K_{t'}$ + 38 K_R + 27 H_ϕ	C−C stretch. +sym. C−N stretch.
C−N			/	1221	1215						
9a	1177	1179	1177	1179						68 H_ϕ + 18 K_t + 15 $K_{t'}$	C−H bend.
9a			/	1172	1175						
15	1156	1155	1152	1155	1153					88 K_t + 24 $K_{t'}$+ 27 H_ϕ	C−H bend. + C−C stretch.
18b	1115	1116	1119/1107	1117/1116	1106	1107	1119	1167	1117	58 K_t+ 35 H_ϕ	C−H bend. + C−C stretch.
18b	1078	1080	1074	1080	1077					42 K_t + 42 H_ϕ	C−H bend. + C−C stretch.
18a	1026	1028	/	1028						32 H_ϕ + 28 K_t + 16 H_α	ring def. + C−H bend.
18a	/	1024	1027/1010	1025/1024	1010	1008	1022	/	1024	33 $K_{t'}$ + 30 H_ϕ + 25 H_α	ring def. + C−H bend.
1 + 12	992	989	992	989						39 K_t+ 25 H_α+ 12 $K_{t'}$	ring def.
1			891	887							
1	844	828	/	826						33 H_α+ 23 $K_{t'}$+ 21 K_R	ring def.
amine	/	743	/	761/731		/	724	/	764	24 K_R + 17 $H_{\delta'}$+ 17 $H_{\phi'}$	C−N−C bend.
			/	639							
6b	610	615	/	609						63 $H_{\alpha'}$ +15 H_ϕ	ring def.

mode can be regarded as a C−C stretching strongly mixed with C−H in-plane bending. In this range of frequencies, an envelope centered around 1500 cm^{-1} in the infrared spectra of B3, B5, and B7 is observed. The vibrational modes 19a and 19b of the inner and terminal rings are consequently difficult to discern. For the terminal rings, the intense band at 1494 cm^{-1} is attributed to the 19a mode, and that around 1486 cm^{-1} to the 19b mode. These modes are rather sensitive to substitution and are shifted for the inner rings to 1524 and 1450 cm^{-1} for 19a and 19b, respectively. This proposal is made on the basis of the following dynamical calculations.

Pure C−H bending vibrational modes are expected around 1300 cm^{-1}, and in Wilson's convention they are referred as no. 3 and no. 14. Vibration 14, denoted as "Kekule vibration", occurs in benzene as a weak Raman band at 1310 cm^{-1}. The Kekule mode of the outer (monosubstituted) rings gives a weak band pointed at 1293 cm^{-1}. Vibration 3 is forbidden in both the IR and Raman spectra of benzene, and even upon substitution it is rather difficult to detect. Moreover, its frequency range is large: 1253−1331 cm^{-1}. We attribute the weak line located at 1334 cm^{-1} to the vibrational mode 3 of the terminal rings and that around 1308 cm^{-1} to the 3 mode of the inner rings. In infrared spectroscopy, we can notice the presence of a very intense band at 1300 cm^{-1}, whereas no intense band is predicted at this frequency. This band cannot be assigned to a band originating from the vibrations of the amine group. Most probably, it corresponds to a coupling between the mode 14 and the asymmetric C−N stretching vibration. This absorption is shifted toward lower frequencies when the chain length increases and is located at 1310, 1300, 1299, and 1282 cm^{-1} in the infrared spectra of B3, B5, B7, and LB, respectively. It can be therefore treated as a diagnostic of the chain length.

For the model compounds of LB, the intense Raman band located around 1223 cm^{-1} is assigned to the symmetric CNC stretching of the amine group. For the polymeric form, the corresponding band is located at 1219 cm^{-1}, showing only a slight frequency dispersion. In the infrared spectra its asymmetric analogue shows up around 1218 cm^{-1}. A second Raman band, which involves an amine group, is pointed at 1426 cm^{-1}. This line corresponds to the N−H bending deformation.

One of the most intense bands in the Raman spectra of all compounds studied is the band observed at about 1177 cm^{-1}. This line can be regarded as a pure C−H in-plane bending vibration and corresponds to the 9a vibrational mode. When the number of aromatic rings increases, its intensity increases. To the contrary, the CNC stretching vibration intensity drops with the increase of the chain length. This band is of particular importance because it is one of the most intense in the polymers and it also appears to be very sensitive to the chemical character of the ring, as we will see in the following.

Another C−H bending vibrational mode is present at 1159 cm^{-1} in the infrared spectra, and it corresponds to the 15 mode. Vibration 15 is forbidden in both the infrared and Raman spectra of benzene. When substituents are identical, vibration 15 is Raman inactive. Thus, the vibration 15 of the inner rings is not observed, whereas the corresponding modes of the terminal rings are expected to decrease in intensity with the increase of the chain length. Indeed, we can note that this mode is not visible in the Raman spectrum of LB.

(c) Region III: <1100 cm^{-1} (Ring Deformations). At low frequencies (<1100 cm^{-1}) the modes related to the ring deformations (radial skeletal vibrations) are expected together with selected C−H out-of-plane vibrations. These modes are useful for the characterization of the mono- or para-substitution, i.e., for the differentiation between the inner rings and the outer rings. They are also very sensitive to the chain length.

In-Plane Ring Vibrations. The in-plane ring vibrations correspond to the vibrational modes 1, 12, 6a, and 6b. Normal

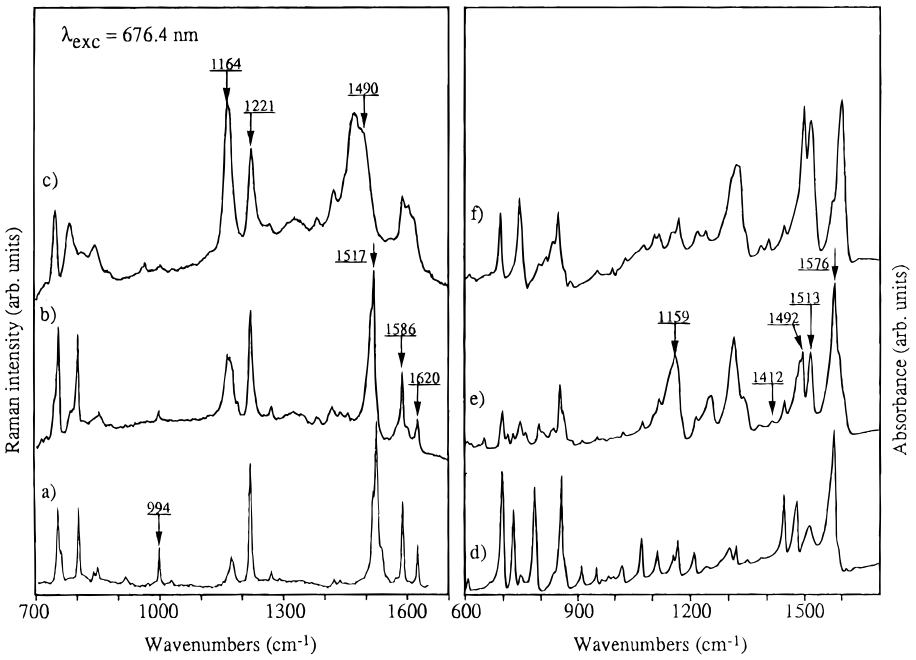

Figure 4. Raman spectra (λ_{exc} = 676.4 nm) of (a) B2Q1, (b) B3Q2, and (c) B4Q1 and infrared spectra of (d) B2Q1, (e) B3Q2, and (f) B4Q1, in the frequency range 700−1650 cm^{-1}.

vibration 1 of benzene is usually referred to as a substituent-sensitive vibration. This vibration falls in the range 1100−1060 cm^{-1} for heavy substituents and in the range 900−620 cm^{-1} for light substituents. Consequently, we assign the Raman band at 882 cm^{-1} to the vibrational mode 1 of the inner rings. It is noteworthy that this mode couples with all sorts of C−X stretching vibrations provided that the latter are of the same symmetry (i.e., 12 and 6b). For light substituents, mode 1 mixes with mode 12 and in terminal rings gives a band at 993 cm^{-1}. This band, called trigonal ring breathing, is always followed by its satellite located at 1028 cm^{-1} (18a). The mode 18a and the mixed mode 1+12 are largely independent of the nature of the adjacent group and are characteristic of monosubstitution. The coupling gives rise to a Raman band which is intense in aniline and gets weaker and weaker as the number of aromatic rings increases to become unobservable in B9.[16] However, we still observe these bands in the Raman spectrum of B7, suggesting that the extent of the conjugation length of the polymeric chain could be at least of eight or nine monomeric units. This conclusion has already been suggested by D'Aprano et al.[20] on the basis of the electrochemical and absorption measurements.

The lowest frequency corresponds to a planar ring deformation, i.e., the 6b CCC bending mode, which is rather insensitive with respect to the substitution. These modes are observed at 620 and 607 cm^{-1} for the outer and inner rings, respectively. The frequency of the 6a ring bending mode in the mono- and para-substituted aromatic rings is quite variable, and consequently, we do not attempt to give any assignment.

Out-of-Plane C−H Deformations. IR out-of-plane C−H wag motions are very suitable for the determination of the type of ring substitution in benzene derivatives. In our case, the two contributions (inner and outer rings) give well separated bands. In the monosubstituted ring, the out-of-plane ring deformation no. 4 occurs as an intense IR band at 693 cm^{-1}. The para-substitution is characterized by an infrared absorption band at 814 cm^{-1}. This band involves the out-of plane deformation vibration 11, where all hydrogens move in-phase and thus give rise to a large dipole moment change and a strong infrared band. The homologous vibration for the monosubstituted rings is observed at 750 cm^{-1}. These three modes are rather substituent-sensitive and may be strongly shifted. They are also present in IR spectra of the oligomers, especially on B7. In the corresponding polymeric form, we observe only the band at 814 cm^{-1}, while the bands at 750 and 693 cm^{-1} disappear. To summarize, we can note that the bands corresponding to the para-disubstituted aromatic ring gain in intensity upon the chain length elongation, whereas the intensity of the bands due to the monosubstituted rings decreases. This observation strongly corroborates our assignment.

B. Oxidized Model Compounds of Polyaniline. Raman and infrared spectra of the model compounds of the basic forms of emeraldine and pernigraniline are shown in Figures 4 and 5.

Before discussing the vibrational spectroscopy results, it is instructive to describe UV−vis−NIR spectra of these compounds[21,22] because strong resonance Raman effects are expected in these cases.

For the oxidized forms of polyaniline, two electronic transitions are registered. The higher energy one at 330 nm is usually ascribed to $\pi \rightarrow \pi^*$ transition. The second band at lower energy has its origin in an excitonic $n \rightarrow \pi^*$ transition involving the benzenoid and quinoid rings. This transition is very sensitive to the oxidation state and leads to strong absorptions, with maxima at 438, 590, and 525 nm in methanol solution for B2Q1, B4Q1, and B3Q2, respectively.

Lu et al.[16] have reported absorption spectra on the longest oligomer, capped octaaniline (referred to as B9 in our nomenclature). They observe a second band centered at 620 nm for "low" oxidation states (B8Q1, B7Q2) and at 525 nm for higher oxidation state (B5Q4). These results obtained for oligomers are in good agreement with previous work. MacDiarmid et al.[23] have shown that in EB and PB the exciton type transitions occur at 640 and 540 nm, respectively. On the basis of the above results, it appears that B2Q1 and B3Q2 should be very good model compounds for the fully oxidized polymer (PB), while B4Q1 could be related to the half-oxidized polymer (EB).

The existence of the visible absorption bands both in the oligomers and in the oxidized forms of the polymer has

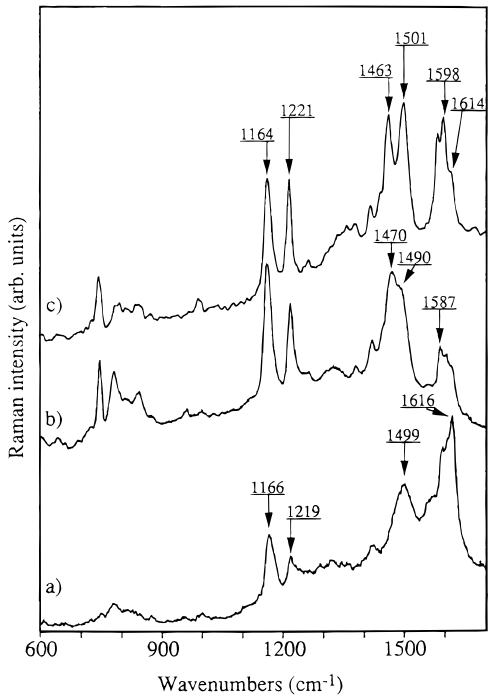

Figure 5. Raman spectra of B4Q1 at different excitation wavelengths: (a) 457.9, (b) 676.4, and (c) 1064 nm.

important influence on their Raman spectra. Due to its resonance effects, bands originating from the oxidized segments should be significantly enhanced if the excitation line energy is close to the energy of the excitonic transition. For this reason, we have used the red excitation line ($\lambda_{exc} = 676.4$ nm) in the studies of EB, PB, and their model compounds.

In this part, we will emphasize the vibrational bands originating from the quinoid ring. Indeed, the vibrational bands related to the aromatic rings are frequently observed at the same frequencies as their analogues in the model compounds of leucoemeraldine base.

We can note that strong resonance effect (frequency shift upon the excitation wavelength) is observed in the Raman spectra of B4Q1, as it is presented in Figure 5. These resonance effects facilitated, in some cases, the assignment of bands. In Tables 3 and 4, the experimental frequencies for oligomer model compound and polymer are collected.

(a) Region I: 3000−3500 cm^{-1}. As in the case of the reduced oligomers, the high frequencies are characteristic of hydrogen stretching modes. In the IR spectrum of B4Q1, C−H and N−H stretching modes are observed around 3050 and 3380 cm^{-1}, respectively. In the IR spectra of B2Q1 and B3Q2 containing imine sites, only the bands to C−H stretchings are present.

(b) Region II: 1100−1700 cm^{-1} (CC Stretching−C−H Bending Vibrations). In the frequency range around 1600 cm^{-1}, one can notice the presence of two well-resolved bands in the Raman spectra: at 1620/1586 cm^{-1} in B3Q2 and 1622/1586 cm^{-1} in B2Q1.

The band at lower frequency (at 1586 cm^{-1} in the Raman spectra of B2Q1 and B3Q2) is resonantly enhanced and for this reason has been assigned to the quinoid ring. This band is due to the C═C stretching mode of the quinoid ring. In the spectrum of B4Q1, similar bands are observed, but they form a broad envelope centered at 1600 cm^{-1}. Several components can then be distinguished at 1588, 1606, and 1614 cm^{-1}. The band at 1588 cm^{-1} has been assigned to the C═C stretching of the quinoid ring. This behavior suggests a higher degree of delocalization in B4Q1. Similar effects are found for the polymers. If the red excitation wavelength is applied, a sharp peak centered at 1579 cm^{-1} is observed in PB, while a large band is centered at the same frequency in EB.

The highest intensity Raman line pointed at ca. 1620 cm^{-1} corresponds to the vibrational mode 8a (CC stretching) of the aromatic rings. The 8b mode, which can also be considered as a C−C stretching mode, gives a weak band located at 1604 cm^{-1} in the Raman spectrum of B2Q1. This mode is not visible in the Raman spectra of the other compounds. We can notice that its frequency is very dependent on the chemical nature of the ring. Indeed, its analogue originating from the quinoid ring (i.e., C−C stretching) gives a weak band at 1416 cm^{-1} in B4Q1 and in B3Q2 and at 1415 cm^{-1} in B2Q1.

In this frequency range, the infrared spectra are characterized by an intense absorption pointed at 1576 cm^{-1} in B3Q2 and in B2Q1 and at 1594 cm^{-1} in B4Q1. This absorption has its origin in a vibrational mode involving the quinoid ring (C═C stretching partly mixed with C−H bending). Several shoulders at high and low frequencies can be distinguished which are associated with the vibrational modes 8a or 8b of the aromatic rings asymmetric with regard to the symmetry center (see Table 4). The characteristic infrared band at about 1580 cm^{-1} is assigned to the quinoid unit, while the band near 1500 cm^{-1} is attributed to the C−C aromatic ring stretching. The intensity ratio of these two absorptions is indicative of the extent of the oxidation. According Wei and co-workers,[19] this ratio is about 80% for EB and decreases by 4-fold to about 20% for LB.

The infrared spectra are also characterized by strong absorptions around 1450−1520 cm^{-1}. Two bands of medium intensities are present at 1478 and 1443 cm^{-1} in B2Q1, whereas in B4Q1 and B3Q2 several lines are observed. The expected vibrations in this region are asymmetric C═N stretching, CC stretching + CH bending, and, generally weak, NH bending modes. However, only one strong absorption is seen in the IR spectra of polymers: 1488 cm^{-1} in PB, 1494 cm^{-1} in EB, and 1496 cm^{-1} in LB. This band is getting more intense, compared to the band at 1580 cm^{-1}, as the oxidation state increases. Thus, we have assigned this absorption to C−C stretching partly mixed with C−H bending in the benzenoid ring. These contributions are strongly mixed with C═N stretching in the case of the oxidized forms of polyaniline and their model compounds. The detailed assignments of these frequencies are proposed in Table 4.

In the Raman spectra, the most intense line is pointed at 1517 cm^{-1} in B3Q2 and in B2Q1. This band is not present in the spectra of the reduced oligomers and should be characteristic of the oxidized state. Consequently, this mode is related, without ambiguity, to the C═N stretching mode. Our assignment is supported by clear enhancement of the band intensity if the excitation line is changed from blue to red (see Figure 5). In the Raman spectrum of B4Q1, the presence of the two isomers is evidenced by the broadness of the band whose maximum is centered at 1475 cm^{-1}. Two components at 1470 and 1489 cm^{-1} can be distinguished. We assign the highest one at 1489 cm^{-1} to the preponderant B4Q1, i.e., the isomer where the central ring possesses a quinoid character. The other component at 1470 cm^{-1} is then related to the C═N stretching of the B4Q1, which possesses its quinoid ring adjacent to the terminal ring. This C═N stretching vibration gives additionally an intense Raman line at 1480 cm^{-1} in pernigraniline base and at 1468 cm^{-1} in emeraldine base, with a significant dispersion effect upon the excitation wavelength in both cases.

TABLE 3: Experimental and Calculated Raman Band Wavenumbers/cm^{-1} of Emeraldine and Pernigraniline Base and Their Model Compounds (Excited at 676.4 nm), PED of B2Q1, and Vibrational Assignment of the Raman Bands

Wilson	B2Q1 A_g		B3Q2 A_g		PB A_g		B4Q1 A_g		EB	PED (%)	
notation	expt	calc	expt	calc	expt	calc	expt	calc	expt	obtained on B2Q1	vibrational assignment
8a			1620	1612	1612	1613	1606	1606			
8a	1620	1622	/	1610			1614	1611		56 K_t + 28 H_ϕ + 14 $K_{t'}$	C−C stretch. ring (B)
8b	1604	1608	/	1605			/	1607		37 K_t + 21 $K_{t'}$ + 36 H_ϕ	C−C stretch. ring (B)
8b				1603	/	1603	/	1626			
	1586	1586	1586	1585	1579	1584	1588	1586	1595	74 K_{QD} + 11 $H_{Q1\phi}$	C═C stretch. ring (Q)
			1568	1570							
19a							1490	1522	1491		
C═N,19a	1517	1515	1517	1511						40 $KQ_{R'}$ + 30 H_ϕ + 13 K_{QR}	C═N stretch. + C−H bend. (B)
19a							/	1502			
C═N			1513	1498	1480	1497	1470	1498	1465		
C═N,19a	1492	1489	/	1487						48 $KQ_{R'}$ + 35 H_ϕ + 10 $K_{t'}$	C═N stretch. + C−H bend. (B)
19b	1447	1463	1454	1459			/	1461		49 H_ϕ + 25 K_t	C−H bend. + C−C stretch. (B)
19b							1449	1445			
N−H							/	1428			
	1415	1416	1416	1415	1418	1416	1421	1409	1419	64 K_{Qt} + 13 $H_{Q\alpha}$ + 10 $H_{Q1\phi}$	C−C stretch. ring (Q)
			1383	1366							
3	1321	1330	/	1331			/	1332		96 H_ϕ + 14 K_t	C−H bend. (B)
			/	1309							
3			/	1304	/	1308	/	1310			
14	1287	1295	/	1282			/	1287		46 H_ϕ + 39 $K_{t'}$ + 22 K_t	C−H bend. (B)
	1261	1262	1264	1261	/	1262	1262	1272		43 $H_{Q1\phi}$ + 20 $H_{Q\phi}$ + 11 H_ϕ	C−H bend. (Q)
C−N							/	1251			
14							/	1248			
C−N	1214	1219	1214	1222/1210	1215	1208	1221	1226/1212	1220	39 K_{QR} + 17 H_ϕ + 12 $H_{Q1\phi}$	C−N stretch.
9a	1172	1176	1184	1180				1180		64 H_ϕ + 23 K_t	C−H bend. (B)
9a			1170	1171	/	1171	/	1171			
	1157	1161	1161	1161	1157	1160	1164	1161	1164	51 $H_{Q1\phi}$ + 19 $H_{Q\phi}$ + 17 K_{QD}	C−H bend. (Q)
15	sh.	1145	/	1157			/	1155		71 K_t + 35 H_ϕ − 22 $F^o_{(t,t)}$	C−H bend. (B)
			/	1107			/	1116			
18b	1100	1080	/	1081			/	1081		45 K_t + 41 H_ϕ	C−H bend. (B)
18a	1024	1024	/	1028			/	1037/1032		33 H_ϕ + 31 K_t + 14 H_α	C−H bend. + ring def. (B)
1 + 12	997	988	996	988			/	992		41 K_t + 23 H_α + 15 $K_{t'}$	C−H bend. + ring def. (B)
			/	951							
1			/	899	/	901	/	900			
	841	840	/	837			/	825		31 H_α + 19 $K_{t'}$ + 15 K_{QR}	ring def. (B)
	794	787	800	790	788	793	783	795	780	66 K_{Qt}	ring def. (Q)
						/	748	749	747		
			/	745							
imine	/	670	/	680	/	690	/	678		29 $H_{Q\delta'}$ + 17 H_α + 13 $H_{Q\alpha}$	C−N═C bend.
6b			/	622				615			
6b	609	604	/	606	/	608	/	600		61 H_α + 15 H_ϕ	ring def. (B)
	588	587	/	586	/	586	/	591		48 $H_{Q\alpha}$ + 27 K_{Qt}	ring def. (Q)

As in the reduced model compounds, in B4Q1, B3Q2, and B2Q1 the Raman-active bands due to symmetric stretching of C−N simple bonds are located at 1214 cm^{-1}. The position of this band is essentially independent of the chain length, contrary to the C═N stretching case. In the infrared spectra, the peaks due to asymmetric corresponding C−N and C═N stretchings are located at 1214 and 1513 cm^{-1}, respectively.

In B2Q1, B3Q2, and B4Q1, the C−H bending mode is located at about 1160 cm^{-1}. In all Raman spectra, this band is very broad. This is due to the fact that in this zone C−H bendings of the aromatic rings (9a) and of the quinoid rings are very close in frequency as well as the vibrational mode 15 of the terminal rings. The mode involving mainly C−H bending originating from the quinoid rings is slightly downshifted with regard to the similar one of the benzenoid ring (9a). We assign the band at low frequency (1166 cm^{-1}) to the C−H bending of the quinoid ring and its shoulder at high frequency to the vibrational mode 9a corresponding to the aromatic rings.

(c) Region III: <1100 cm^{-1} (Ring Deformations). In this zone, the modes associated with the ring vibrations are numerous. The Raman features of the monosubstituted rings (see previous part on reduced oligomer) can be easily distinguished at ca. 997 and 1024 cm^{-1} in the Raman spectra of B2Q1 etc. Raman spectra are also characterized by two bands pointed at about 802 and 752 cm^{-1}, assigned respectively to the ring breathing of the quinoid ring and to the imine deformations. The band at ca. 846 cm^{-1} is due to the amine deformations. The bands in IR spectra are numerous in this frequency range. Consequently, it is rather difficult to differentiate between the out-of-plane vibrational modes and the in-plane vibrational modes. The same applies to the bands of aromatic and quinoid rings. The assignments of these bands will be proposed in the following section.

4. Vibrational Calculations. One of the main purposes of this vibrational analysis consists not only in clearing up some doubts about the assignment of the vibrational modes of the base forms of polyaniline and their model compounds but also in obtaining the two extreme sets of force constants related to the reduced and oxidized structures schematically depicted in Figure 6.

In Tables 1, 2, 3, and 4, experimental and calculated frequencies of the base forms of polyaniline and their model compounds have been reported. On the basis of in-plane valence-force-field calculations, two sets of parameters that describe the electronic configuration of the polymeric forms have been obtained. These two force-fields are given in Tables

TABLE 4: Experimental and Calculated Infrared Band Wavenumbers/cm^{-1} of Emeraldine and Pernigraniline Base and Their Model Compounds (Excited at 676.4 nm), PED of B2Q1, and Vibrational Assignment of the Infrared Bands

Wilson	B2Q1 B_u		B3Q2 B_u		PB B_u		B4Q1 B_u		EB	PED (%)	
notation	expt	calc	expt	calc	expt	calc	expt	calc	expt	obtained on B2Q1	vibrational assignment
8b							/	1625			
8a							/	1606			
8a	/	1622	1602	1610			/	1607		56 K_t + 28 H_ϕ + 14 $K_{t'}$	C−C stretch. ring (B)
8b	/	1607	/	1605			/	1611		38 K_t + 36 $K_{t'}$ + 22 H_ϕ	C−C stretch. ring (B)
			1588	1586							
	1576	1570	1576	1570	1571	1572	1594	1570	1590	79 K_{QD} + 12 $H_{Q1\phi}$	C═C stretch. ring (Q)
C═N, 19a				1524	/	1525	1513	1522			
C═N, 19a	1512	1516	1513	1511						45 $KQ_{R'}$ + 29 H_ϕ+ 14 K_{QR}	C═N stretch. + C−H bend. (B)
19a							/	1502			
C═N, 19a			1492	1490	1488	1490	1494	1499	1494		
C═N, 19a	1478	1489	1485	1487						47 $KQ_{R'}$ + 36 H_ϕ + 11 $K_{t'}$	C═N stretch. + C−H bend. (B)
19b	1443	1461	1477	1459			/	1461		52 H_ϕ + 27 K_t	C−H bend. + C−C stretch. (B)
19b			1445	1437	1412	1433	1443	1441	1445		
N−H							/	1427			
			1412	1411							
	1384	1368	1380	1367	1377	1367	1381	1368	1378	53 K_{Qt} + 12 $H_{Q\phi'}$	C−C stretch. (Q)
3	1334	1329	1337	1331			/	1332/1305		95 H_ϕ + 15 K_t	C−H bend. (B)
	1302	1308	1311	1308	1315	1308	/	1309		68 $H_{Q1\phi}$ + 19 $H_{Q\phi}$+ 18 K_{Qt}	C−H bend. (Q)
14	1286	1286	/	1284			1289	1283		50 H_ϕ+ 44 $K_{t'}$ + 20 K_t	C−H bend. (B)
			1255	1268			/	1258			
14			/	1250	/	1254	/	1249			
C−N			/	1230					1237		
C−N	1212	1224	1215	1220	1211	1234	1238/1217	1229/1216	1216	47 K_{QR}+ 19 H_ϕ + 10 H_α	sym. C−N stretch.
9a	1168	1176	1178	1180			1168	1180/1172		64 H_ϕ + 23 K_t	C−H bend. (B)
			1159	1161							
15	1150	1147	/	1157			1152	1155		68 K_t + 35 H_ϕ − 20 $F^o_{(t,t)}$	C−H bend. (B)
18b			1119	1118	/	1118	1117	1116			
	1114	1107	1106	1106	1100	1105	1105	1106	1103	44 $H_{Q1\phi}$ + 17 K_{QD} + 14 K_{Qt}	C−H bend. (Q)
18b	1072	1080	1075	1081			1077	1081		44 K_t + 41 H_ϕ	C−H bend. (B)
18a	1020	1024	/	1028				1037		33 H_ϕ + 31 K_t + 14 H_α	C−H bend. + ring def. (B)
18a			1023	1025	1006	1025	1028	1032			
1 + 12	997	988	998	988			993	992		40 K_t + 23 H_α + 14 $K_{t'}$	ring def. (B)
	951	951	952	951	954	950	952	951	955	38 $H_{Q\alpha}$ + 20 $K_{Q\phi}$ + 17 K_{Qt}	C−H bend. + ring def. (Q)
1							879	898			
	835	833	858	837			832	824	828	33 H_α + 20 $K_{t'}$ + 16 K_{QR}	C−H bend. + ring def. (Q)
			794	789							
			759	763	750	760	/	736			
	746	740	726	733	/	727	/	758		47 K_{Qt} + 18 $H_{Q\delta'}$+ 14 $H_{Q\alpha'}$	C−N═C bend.
6b		618	616	604			611	639/603		58 H_α + 14 H_ϕ	ring def. (B)

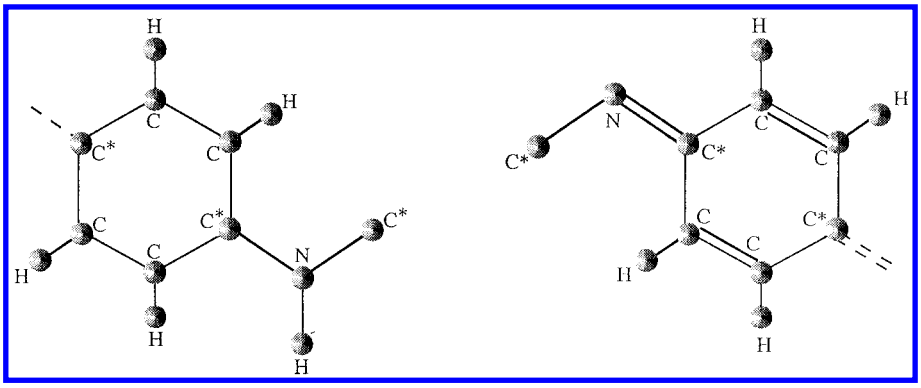

Figure 6. Schematic representation of the reduced and oxidized units.

5 and 6. To confirm the proposal of assignment, the potential energy distributions (PED) have been calculated. They are collected in Tables 1 and 2 for B3 and in Tables 3 and 4 for B2Q1.

A. Wilsonian Matrix. Calculated frequencies and suitable valence force field have been obtained by the use of a dynamic model, using force constants defined by eq 1.

$$F_{RR'} = \left(\frac{\partial^2 \phi}{\partial R\, \partial R'}\right)_0 \qquad (1)$$

where ϕ represents the potential energy and R, R′ two internal coordinates. Indeed, these force constants have the most direct physical meaning when written in terms of internal coordinates (bond stretching and angle bending).

Preliminarily, some hypothesis are made:

(i) We consider a planar geometry of the ring, which permits separating in-plane and out-of-plane modes. In our study, the calculations concern only the in-plane vibrational modes.

(ii) We assume also that the force constants are fairly local: they are only dependent on the location and the type of the few nearest neighbors.

TABLE 5: Force Constants of the Reduced Units

symbol	coordinates involved	common atoms	value of the force constants
	Diagonal Force Constants: Stretch (mdyn Å^{-1})		
K_s	C−H	/	5.09
$K_{s'}$	N−H	/	6.21
K_t	C−C	/	6.21
$K_{t'}$	C−C*	/	6.32
K_R	C*-N	/	5.32
	Diagonal Force Constants: Bend (mdyn Å rad^{-2})		
H_ϕ	∠CCH and ∠C*CH	/	0.50
H_α	∠CCC and ∠C*CC	/	1.04
H_δ	∠C*NH	/	0.68
$H_{\phi'}$	∠CC*N	/	0.86
$H_{\alpha'}$	∠CC*C	/	1.17
$H_{\delta'}$	∠C*NC*	/	1.21
	Interaction Constants: Bend−Bend (mdyn Å rad^{-2})		
$F_{(\alpha,\alpha)}$	∠CCC, ∠CCC	C−C	0
$F_{(\phi,\phi)}$	∠CCH, ∠CCH	C−C	0.02
$F_{(\alpha,\alpha')}$	∠CCC*, ∠CC*C	C−C*	0.15
$F_{(\phi',\delta)}$	∠CC*N, ∠C*NH	C*−N	0.25
$F_{(\phi',\delta')}$	∠CC*N, ∠C*NC*	C*−N	0.12
	Interaction Constants: Stretch−Stretch (mdyn Å^{-1})		
$F_{(s,t)}$	C−H, C−C and C−H, C−C*	C	0
$F^{o}_{(t,t)}$	C−C, C−C	C or C*	0.80
$F^{m}_{(t,t)}$	C−C, C−C	/	−0.38
$F^{p}_{(t,t)}$	C−C, C−C	/	0.33
$F_{(t',R)}$	C−C*, C*-N	C*	0.46
$F_{(R,s')}$	C*-N, N−H	N	−0.31
$F_{(R,R)}$	C*-N, C*-N	N	0.72
$F_{(t',s')}$	C*-C, N−H	/	0.27
	Interaction Constants: Stretch−Bend (mdyn rad^{-1})		
$F_{(s,\alpha)}$	C−H, ∠CCC	C	−0.13
$F_{(t,\alpha)}$	C−C, ∠CCC	C−C	0.11
$F_{(t,\phi)}$	C−C, ∠CCH	C−C	0.16
$F_{(t',\alpha')}$	C−C*, ∠CC*C	C−C*	0.36
$F_{(t',\phi')}$	C−C*, ∠CC*N	C−C*	0.30
$F_{(R,\alpha')}$	C*-N, ∠CC*C	C*	−0.13
$F_{(R,\delta)}$	C*-N, ∠C*NH	C*−N	0.36
$F_{(R,\delta')}$	C*-N, ∠C*NC*	C*−N	0.44
$F_{(s',\delta')}$	N−H, ∠C*NC*	N	0.07

TABLE 6: Force Constants of the Oxidized Units

symbol	coordinates involved	common atoms	value of the force constants
	Diagonal Force Constants: Stretch (mdyn Å^{-1})		
K_{QD}	C=C	/	8.24
K_{Qt}	C−C*	/	4.51
K_{QR}	C*−N	/	5.24
$K_{QR'}$	C*=N	/	9.10
	Diagonal Force Constants: Bend (mdyn Å rad^{-2})		
$H_{Q\phi}$	∠C*−C−H	/	0.29
$H_{Q1\phi}$	∠C=C−H	/	0.62
$H_{Q\phi'}$	∠C−C*=N	/	0.89
$H_{Q\alpha}$	∠C*−C=C	/	1.06
$H_{Q\alpha'}$	∠C−C*−C	/	0.64
$H_{Q\delta'}$	∠C*=N−C*	/	1.78
	Interaction Constants: Stretch−Stretch (mdyn Å^{-1})		
$F_{(QR,t')}$	C*−N, C−C*	C*	0.62
$F_{(QR,QR')}$	C*−N, C*=N	N	0.54
$F_{(Qt,QR')}$	C−C*, C*=N	C*	0.53
$F_{(s,Qt)}$	C−H, C−C*	C	0.05
$F_{(s,QD)}$	C−H, C=C	C	−0.06
$F^{p}_{(QD,QD)}$	C=C, C=C	/	0.05
$F^{o}_{(QD,Qt)}$	C=C, C−C*	C	0.35
$F^{m}_{(QD,Qt)}$	C=C, C−C*	/	−0.06
$F^{o}_{(Qt,Qt)}$	C−C*, C−C*	C*	0.21
	Interaction Constants: Bend−Bend (mdyn Å rad^{-2})		
$F_{(Q1\phi,Q1\phi)}$	∠C=C−H, ∠C=C−H	C=C	0.07
$F_{(Q\phi',Q\phi)}$	∠C−C*=N, ∠C*−C−H	C−C*	−0.11
$F_{(Q\alpha,Q\alpha)}$	∠C*−C−C, ∠C*−C−C	C=C	0.03
$F_{(Q\alpha,Q\alpha')}$	∠C*−C−C, ∠C−C*−C	C−C*	−0.07
$F_{(\phi',Q\delta')}$	∠CC*N, ∠C*=N−C*	C*−N	0.19
$F_{(Q\phi',Q\delta')}$	∠C−C*=N, ∠C*=N−C*	C*=N	−0.01
	Interaction Constants: Stretch−Bend (mdyn rad^{-1})		
$F_{(Qt,Q\alpha)}$	C−C*, ∠C*−C−C	C−C*	0.12
$F_{(Qt,Q\alpha')}$	C−C*, ∠C−C*−C	C−C*	0.49
$F_{(Qt,Q\phi)}$	C−C*, ∠C*−C−H	C−C*	0.26
$F_{(Qt,Q\phi')}$	C−C*, ∠C−C*=N	C−C*	0.20
$F_{(QD,Q\alpha)}$	C=C, ∠C*−C−C	C=C	0.54
$F_{(QD,Q1\phi)}$	C=C, ∠C=C−H	C=C	0.08
$F_{(QR,\alpha')}$	C*−N, ∠CC*C	C*	−0.08
$F_{(QR,Q\delta')}$	C*−N, ∠C*=N−C*	C*−N	0.61
$F_{(QR',Q\delta')}$	C*=N, ∠C*=N−C*	C*=N	0.53
$F_{(QR',Q\alpha')}$	C*=N, ∠C−C*−C	C*	−0.97
$F_{(s,Q\phi)}$	C−H, ∠C*−C−H	C−H	0.01
$F_{(s,Q1\phi)}$	C−H, ∠C=C−H	C−H	0.08

(iii) The polymers are described as perfect infinite chains containing no defects.

The calculating procedure is as follows:

(i) First, a starting set of force constants is chosen using previous results on benzene and diphenylamine in the case of the reduced model compounds and *p*-benzoquinone[24,25] in the case of the oxidized units.

(ii) Then, the difference between each calculated frequency and the corresponding observed frequency is refined by a least-squares-fitting procedure where the standard deviation *X* given by eq 2 is minimized.

$$X = \left[\frac{1}{N}\sum_{i=1}^{N}(\omega^{i}_{exp} - \omega^{i}_{cal})^2\right]^{1/2} \qquad (2)$$

where ω^{i}_{exp} and ω^{i}_{cal} are respectively the observed and calculated frequencies of the vibration i and N is the number of observed frequencies.

(iii) Step (ii) is repeated until the standard deviation *X* reaches a minimum. We can note that changes of the force constants must be limited in order to control a wrong evolution, which may lead to nonphysical values at the end of the iteration.

Finally, a clear assignment of the vibrational modes is obtained by the study of the potential energy distribution (PED), which allows the fractional part of the potential energy of a normal mode of vibration contributed by each force constant.

B. Practical Considerations. Let us remark on some important practical considerations.

(i) Raman and infrared data of B7 have not been included in the refinement because the observed frequencies are not numerous enough compared to the number of predicted experimental modes.

(ii) The exclusion rule between IR and Raman modes has been evidenced on the spectra of B4Q1. Then, we have to consider that we have mainly characterized the isomer BBQBB.

For this reason, this isomer is the only form of B4Q1 that has been taken into account in our calculations.

(iii) The modes at high frequency (N−H and C−H stretching) have also not been taken into account during the refinement because they become less and less discernible with the increase of the chain length.

C. Group Theory. The group theory is an interesting tool to predict, among other things, the Raman and infrared activity of the bands. In the hypothesis of planar molecules, all the reduced model compounds of leucoemeraldine base (B3, B5, and B7) belong to the same point group C_{2h}, whereas the corresponding polymeric form (LB) possesses $D_{2h}(q=0)$ symmetry. In the 0−1700 cm^{-1} spectral range, 53, 91, and 125 fundamental in-plane vibrational modes are active in B3, B5, and B7, respectively. In the C_{2h} structure, the 53 fundamental in-plane vibrational modes of B3 can be separated into 27 A_g and 26 B_u vibrations, and the 91 fundamental in-plane vibrational modes of B5 can be separated into 46 A_g and 45 B_u vibrations. In the case of the leucoemeraldine base, they are reduced to 9 A_g, 10 B_{3g}, 8 $B_{1u,}$ and 9 B_{2u} vibrations.

All the oxidized molecules under study possess C_{2h} symmetry except the BQBBB form of B4Q1 which possess C_s symmetry. The corresponding polymeric forms, emeraldine and pernigraniline base belong to the $C_{2h}(q=0)$ point group. At low frequency (<1700 cm^{-1}), 51, 89 and 87 fundamental in-plane vibrational modes are active in B2Q1, B4Q1 (BBQBB) and B3Q2, respectively. In the C_{2h} structure, these fundamentals in-plane vibrational modes are separated into 26 A_g and 25 B_u vibrations for B2Q1, into 45 A_g and 44 B_u vibrations for BBQBB and into 44 A_g and 43 B_u vibrations for B3Q2. In the case of the oxidized forms of polyaniline, the in-plane vibrational modes can be decomposed as follows: 41 A_g and 41 B_u for EB and 18 A_g and 16 B_u for PB.

Let us remind that the presence of a center of symmetry in these molecules and macromolecules induces the mutual exclusion of the activity of infrared and Raman bands. Moreover, the modes with "gerade" symmetry are allowed in Raman spectroscopy and forbidden in infrared whereas it is the contrary for the modes with "ungerade" symmetry.

D. Geometrical Values. Dynamical calculations have been performed using geometric parameters obtained from literature.[26,27] The same values have been taken for all the model compounds and for the corresponding polymer. Bond lengths have been taken as follows: $r(C-C)_{\text{aromatic ring}} = 1.41$ Å, $r(C-H)_{\text{ring}} = 1.06$ Å, $r(C=C)_{\text{quinoid ring}} = 1.36$ Å, $r(C-C)_{\text{quinoid ring}} = 1.49$ Å, $r(C-N) = 1.42$ Å, $r(C=N) = 1.30$ Å, and $r(N-H) = 1.01$ Å. Bond angles have been chosen (for both the aromatic rings and the quinoid rings) equal to the idealized 120°. In our calculations, as suggested by the geometry proposed by Baughman et al.[28] relative to the ClO_4^- and BF_4^- cation salts of the dimer, the C−N−C bond angle has been modified to 130°. No notable differences have been obtained; that is why the C−N−C bond angle has also been taken equal to the idealized 120°.

E. Assignment. Using a suitable valence force field, the calculated frequencies appeared in good agreement with the experimental ones. The values collected are shown in Tables 1, 2, 3, and 4. For more simplicity, we will discuss the force constants separately.

(a) C−C Stretching Vibrations (1650−1300 cm^{-1}). In this region, for the reduced units the C−C stretching character gives vibrational modes 8a and 8b calculated around 1600 cm^{-1}, as expected. The PED of 8a and 8b modes are very similar and reveal a ca. 70% C−C stretching character, for all compounds. However, we can note that the preponderant character of the higher mode (8a) is given by K_t and the dominant character of the shoulder (8b) is provided by the C−C stretching perturbed by the amine group ($K_{t'}$). These modes very close in frequency (8a and 8b) in the reduced model compounds split into two well-defined bands in the oxidized model compounds. The C=C stretching (75%) gives a Raman band calculated at 1584 cm^{-1}. The other component relative to the C−C stretching (K_{Qt}) falls to the calculated value of 1422 cm^{-1}. These components are particularly interesting because the difference between the related force constants K_t and $K_{t'}$ in the case of the reduced model compounds and K_{QD} and K_{Qt} in the case of the oxidized model compounds is characteristic of the nature of the ring.

In the infrared spectra, the C−C stretching component (about 30%) strongly mixed with 60% of C−H bending gives bands assigned previously to the vibrational modes 19a and 19b. They also represent the nature of the ring. Indeed, these modes give rise to a broad intense absorption located around 1500 cm^{-1} in the reduced compounds. In the fully oxidized compounds, these modes are included in an intense absorption located at about 1570 cm^{-1}. Consequently, the intensity ratio of these two contributions are directly related to the oxidation state of the molecules or macromolecules under study. We can note that it seems very difficult to ensure our assignment in this frequency range for the reduced structure, even after the vibrational analysis.

(b) C−H Bending Vibrations (1300−1100 cm^{-1}). In this region, calculated frequencies are in rather good agreement with experimental ones. We focused our interest on the intense band pointed at 1181, 1166, and 1157 cm^{-1} in the Raman spectra of the leucoemeraldine, emeraldine, and pernigraniline, respectively. These modes possess a strong C−H bending character and are calculated at 1171 cm^{-1} (55% of C−H bending character) in LB and at 1161 cm^{-1} (50% of $H_{Q1\phi}$) in the fully oxidized model compounds and PB. In the Raman spectrum of EB, these two contributions are mixed, leading to a broad band at about 1166 cm^{-1}. Consequently, the sharpness and the frequency of this Raman mode can also be a criteria of the oxidation state. The small shifts are probably due to the steric environment, which is not taken into account in our planar model, for the reduced structures. Indeed, the planarity of the oxidized model compounds and in particular B3Q2 leads to better calculated values. Similar problems have been encountered previously for the vibrational modes 19a and 19b, which also possess a strong C−H bending component.

(c) Ring Vibrations (1100−600 cm^{-1}). In benzene, the ring breathing (mode 1) is considered a pure C−C stretching mode. Upon substitution, the vibrational mode 1 of the inner rings lost a part of its strong C−C character for the benefit of the C−N stretching component (13%). The calculated values are 872 and 796 cm^{-1} in LB (aromatic) and PB (quinoid), respectively. These frequencies are in good agreement with the observed, which are pointed at 868 and 788 cm^{-1} in LB and PB, respectively. On the contrary, its homologous relative to the inner rings, i.e., the vibrational mode 1+12 calculated at 989 cm^{-1}, keeps its strong C−C stretching character (65%), which is in agreement with the fact that this mixing (1+12) should be less perturbed by the substitution.

(d) In-Plane Vibrational Modes of the Amine and Imine Groups. The calculated values of the modes from the amine and imine groups are in good agreement with the experimental ones. The vibrational mode calculated at 1423 cm^{-1} has about 93% N−H bending character. Two bands pointed at 1220 and 1253 cm^{-1} are associated with the amine group, and they possess, as predicted, a strong C−N stretching character. The

asymmetric (1253 cm^{-1}) and symmetric (1220 cm^{-1}) C−N stretching have 44 and 69% C−N stretching character, respectively. In the oxidized model compounds, the C═N stretching character mixes with other modes relative to the outer rings (19a and 19b); the preponderant C═N stretching is obtained for the 1480 cm^{-1} calculated value. In the polymeric form PB, this vibrational mode is highly pure.

F. Force Constants. On the basis of these considerations, a valence force field, i.e., a set of force constants expressed in terms of internal coordinates, has been built for both the reduced and the oxidized structures. The two sets of force constants (Tables 5 and 6) have been optimized on a very large number of molecules and polymers, i.e., a large number of experimental frequencies. These force constants are in accordance with the base forms of polyaniline and their model compounds under our disposal and are more coherent consequently than those reported in previous similar works.[5,29] The slight discrepancies between all these sets are due to the number of molecules under investigation and the small shifts between geometrical parameters.

Our sets of force constants can be divided into two different groups: those associated with the diagonal force constants and those associated with the interaction force constants. In the frame of our model, we used 33 force constants to interpret the experimental frequencies of the reduced unit and 56 force constants to interpret the experimental frequencies of the oxidized unit. Among these 56 parameters 19 have been directly transferred from the reduced part.

Among all these parameters, one can consider that the diagonal force constants play a more important role, particularly those associated with the carbon−carbon and carbon−nitrogen bonds, since they are directly related to the electronic structure of the compounds. The carbon−carbon parameters are found physically reasonable according to the nature of the bond. Indeed, $K_t = 6.03$ mdyn/Å and $K_{t'} = 6.32$ mdyn/Å (reduced structure) and $K_{QD} = 8.23$ mdyn/Å and finally $K_{Qt} = 4.64$ mdyn/Å (oxidized structure) reveal double and simple character, respectively. Concerning carbon−nitrogen bonds, a reasonable agreement between observed and calculated frequencies has also been obtained with the following values: $K_R = 5.33$ mdyn/Å for the reduced units and $K_{QR} = 5.16$ mdyn/Å and $K_{QR'} = 9.22$ mdyn/Å in the case of the oxidized ones. We can notice that these values are very interesting because they reveal the changes induced by the oxidation on the amine/imine group.

We can notice that these two sets are in good consistency with the bond lengths, and they are completely transferable from one molecule to the other. They represent the vibrational fingerprint and the electronic configuration of the reduced and oxidized structures. Moreover, the error between the observed and calculated frequencies given by eq 2 is 10.3 cm^{-1} in the case of the reduced model compounds and 9.1 cm^{-1} in the case of the oxidized ones. Consequently, this reasonable agreement suggests that the effect of planar geometry is not significant on in-plane vibrational assignments above 900 cm^{-1}. Moreover, Kertesz and Choi[29] have shown that the best agreement between the calculated spectra and the Raman experiments can be achieved for planar models of LB.

5. Conclusion

In this paper, a detailed investigation of the vibrational properties of the base forms of polyaniline has been performed by the use of a model compounds approach. Calculated frequencies and two sets of force constants traducing the reduced and oxidized structures have been obtained by an in-plane valence-force-field model. The values of these force constants are physically reasonable and completely consistent with the nature of the ring (aromatic or quinoid). Because of the extension of the chain length, our previous assignments have been confirmed and the two obtained sets of force constants should be a little better than those reported by S. Quillard et al.

Similar studies on model compounds of emeraldine salt are in progress in order to determine the vibrational modifications induced by the doping and to obtain electronic structure of emeraldine salt via vibrational calculations and their effect on the obtained set of force constants.

Acknowledgment. The authors would like to thank Professor Adam Prón for useful discussions and PANET for their financial support.

References and Notes

(1) See, for example: Proceedings of the International Conference of Synthetics Metals-Utah July 1996, *Synth. Met.* **1997**, 84.
(2) Sherman, B. C.; Euler, W. B.; Forcé, R. R. *J. Chem. Educ.* **1994**, *71* (4), A94.
(3) Kuo, C.-T.; Chiou, W.-H. *Synth. Met.* **1997**, *88*, 23.
(4) Lu, W.-K.; Elsenbaumer, R. L.; Wessling, B. *Synth. Met.* **1995**, *71*, 2163.
(5) Quillard, S.; Louarn, G.; Lefrant, S.; MacDiarmid, A. G. *Phys. Rev. B* **1994**, *50*, 12496.
(6) Libert, J.; Brédas, J. L.; Epstein, A. J. *Phys. Rev. B* **1995**, *51* (9), 5711.
(7) Louarn, G.; Buisson, J. P.; Lefrant, S.; Fichou, D. *J. Phys. Chem.* **1995**, *99*, 11399; Lefrant, S.; Buisson, J. P. In *Frontiers of Polymers and Advanced Materials*; Prasad, P. N., Ed.; Plenum Press: New York, 1994.
(8) Bäuerle, P. *Adv. Mater. 4* **1992**, *2*, 102.
(9) Furukawa, Y.; Ueda, F.; Hyodo, Y.; Harada, I.; Nakajima, T.; Kawagoe, T. *Macromol.* **1988**, *21*, 1297. Furukawa, Y.; Hara, T.; Hyodo, Y.; Harada, I. *Synth. Met.* **1986**, *16*, 189. Quillard, S.; Louarn, G.; Buisson, J. P.; Lefrant, S.; Masters, J.; MacDiarmid, A. G. *Synth. Met.* **1992**, *49*−*50*, 525.
(10) Cui, C. X.; Kertesz, M. *J. Chem. Phys.* **1993**, *7*, 5257.
(11) Brédas, J. L.; Silbey, R.; Boudreaux, D. S.; Chance, R. R. *J. Am. Chem. Soc.* **1983**, *105*, 6555.
(12) Schaklette, L. W.; Wolf, J. F.; Gould, S.; Baughman, R. H. *J. Chem. Phys.* **1988**, *6*, 3955.
(13) Quillard, S.; Louarn, G.; Buisson, J. P.; Lefrant, S.; Masters, J.; MacDiarmid, A. G. *Synth. Met.* **1992**, *49*−*50*, 525.
(14) Wei, Y.; Yang, C.; Wei, G.; Feng, G. *Synth. Met.* **1997**, *84*, 28.
(15) Honzl, J.; Tlustakova, M. *J. Polym. Sci.: Part C* **1968**, *22*, 451.
(16) Lu, F. L.; Wudl, F.; Nowak, M.; Heeger, A. J. *J. Am. Chem. Soc.* **1986**, *108*, 8311.
(17) Wudl, F.; Angus, R. O.; Lu, F. L.; Allemand, P. M.; Vachon, D. J.; Nowak, M.; Liu, Z. X.; Heeger, A. J. *J. Am. Chem. Soc.* **1987**, *109*, 3677.
(18) Rebourt, E.; Joule, J. A.; Monkman, A. P. *Synth. Met.* **1997**, *84*, 65.
(19) Wei, Y.; Hsueh, K. F.; Jang G. W. *Macromolecules* **1994**, *27*, 518.
(20) D'Aprano, G.; Leclerc, M.; Zotti, G. *Synth. Met.* **1996**, *82*, 59.
(21) Zaghal, M. H.; Shatnawi, M. Y. *Oppi Briefs* **1989**, *21* (3), 364.
(22) Zhang, W. J.; Feng, J.; MacDiarmid, A. G.; Epstein, A. J. *Synth. Met.* **1997**, *84*, 119.
(23) Masters, J. G.; Sun, Y.; MacDiarmid, A. G.; Epstein, A. J. *Synth. Met.* **1991**, *41*−*43*, 715.
(24) Palmö, K.; Pietilä, L.-O.; Mannfors, B.; Karonen, A.; Stenman, F. *J. Mol. Spectrosc.* **1983**, *100*, 368.
(25) Pietilä, L.-O.; Palmö, K.; Mannfors, B. *J. Mol. Spectrosc.* **1986**, *116*, 1.
(26) Stafström, S.; Sjögren, B.; Wennerström, O.; Hjertberg, T. *Synth. Met.* **1896**, *16*, 31.
(27) Langer, J. J. *Synth. Met.* **1987**, *20*, 35.
(28) Baughman, R. H.; Wolf, J. F.; Eckhardt, H.; Shacklette, L. W. *Synth. Met.* **1988**, *25*, 121.
(29) Kertesz, M.; Choi, C. H.; Hong, S. Y. *Synth. Met.* **1997**, *85*, 1073. Choi, C. H.; Kertesz, M. *Macromolecules* **1997**, *30*, 620. Kostic, R.; Davidova, I. E.; Gribov, L. E.; Rakovic, D. *J. Serb. Chem. Soc.* **1990**, *55* (11), 617.